Journal Pre-proof

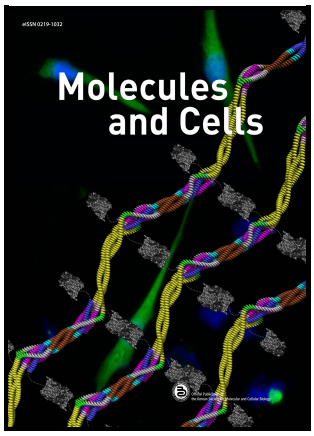


# A FMRFamide-like neuropeptide FLP-12 signaling regulates head locomotive behaviors in *C. elegans*Running title: FLP-12 mediates stomatal oscillation

Do-Young Kim, Kyeong Min Moon, Woojung Heo, Eun Jo Du, Cheon-Gyu Park, Jihye Cho, Jeong-Hoon Hahm, Byung-Chang Suh, KyeongJin Kang, Kyuhyung Kim

PII: S1016-8478(24)00149-3

DOI: https://doi.org/10.1016/j.mocell.2024.100124

Reference: MOCELL100124

To appear in: *Molecules and Cells*

Received date: 10 September 2024
Revised date: 8 October 2024
Accepted date: 13 October 2024

Please cite this article as: Do-Young Kim, Kyeong Min Moon, Woojung Heo, Eun Jo Du, Cheon-Gyu Park, Jihye Cho, Jeong-Hoon Hahm, Byung-Chang Suh, KyeongJin Kang and Kyuhyung Kim, A FMRFamide-like neuropeptide FLP-12 signaling regulates head locomotive behaviors in *C. elegans*Running title: FLP-12 mediates stomatal oscillation, *Molecules and Cells,* (2024) doi:https://doi.org/10.1016/j.mocell.2024.100124

# A FMRFamide-like neuropeptide FLP-12 signaling regulates head locomotive behaviors in *C. elegans*

Running title: FLP-12 mediates stomatal oscillation

Do-Young Kim[1†], Kyeong Min Moon[1†], Woojung Heo[1†], Eun Jo Du[2], Cheon-Gyu Park[1], Jihye Cho[1], Jeong-Hoon Hahm[3], Byung-Chang Suh[1], KyeongJin Kang[2], and Kyuhyung Kim[1, 2]

[1]Department of Brain Sciences, DGIST, Daegu, 42988, Republic of Korea.

[2]KBRI (Korea Brain Research Institute), Daegu, 41068, Republic of Korea.

[3]Aging and Metabolism Research Group, KFRI, Wanju, 55365, Republic of Korea

[*]Corresponding author: Ki.K; khkim@dgist.ac.kr

[†]These authors contributed equally to this work.



## ABSTRACT

Neuropeptides play a critical role in regulating behaviors across organisms, but the precise mechanisms by which neuropeptides orchestrate complex behavioral programs are not fully understood. Here, we show that the FMRFamide-like neuropeptide FLP-12 signaling from the SMB head motor neurons, modulates head locomotive behaviors, including stomatal oscillation in *C. elegans*. *lim-4* mutants, in which the SMB neurons are not properly specified, exhibited various head and body locomotive defects, including stomatal oscillation. Chronic activation or inhibition of neuropeptidergic signaling in the SMB motor neurons resulted in a decrease or increase in stomatal oscillation, respectively. The *flp-12* neuropeptide gene is

expressed and acts in the SMB neurons to regulate head and body locomotion, including stomatal oscillation. Moreover, the *frpr-8* GPCR and *gpa-7* Gα genes are expressed in the AVD command interneurons to relay the FLP-12 signal to mediate stomatal oscillation. Finally, heterologous expression of FRPR-8 either *Xenopus* oocytes or HEK293T cells conferred FLP-12 induced responses. Taken together, these results indicate that the *C. elegans* FMRFamide neuropeptide FLP-12 acts as a modulator of stomatal oscillation via the FRPR-8 GPCR and the GPA-7 G-protein.

Keywords:

*C. elegans, flp-12, frpr-8,* FMRFamide*,* head locomotion



## INTRODUCTION

In many organisms, behaviors ranging from simple reflexes to complex patterns are controlled by intricate neural circuits. Neuropeptides are major signaling molecules that influence neural circuits and, consequently, behavior (Kow and Pfaff, 1988; Sharma et al., 2022). Unlike classical neurotransmitters, which typically act at synaptic sites, neuropeptides can diffuse over longer distances and influence entire networks of neurons, orchestrating a range of complex behaviors, including feeding, social, and sexual behaviors, through their broad and often modulatory effects (Bhat et al., 2021; Kow and Pfaff, 1988; Painsipp et al., 2008; Quillet et al., 2016; Ryu et al., 2022; Sharma et al., 2022). For example, hypothalamic neuropeptide, oxytocin, coordinates multiple social behaviors by conserved but rather distinct cellular and circuit mechanisms (Froemke and Young, 2021). However, despite their importance, the specific

mechanisms by which neuropeptides regulate particular behaviors remain largely unexplored.

In *Caenorhabditis elegans*, a small nematode with a well-characterized nervous system, a variety of simple and complex behaviors has been extensively studied to uncover the fundamental principles of neural circuit structure and function. In *C. elegans*, 113 neuropeptide genes have been identified, encoding more than 250 distinct neuropeptides, including 31 FMRFamide-related peptide genes (FLPs) (Li and Kim, 2014), which may act via at least 149 putative neuropeptide G protein-couple receptor genes. Several *flp* genes function in locomotive behaviors. For example, *flp-1* regulates locomotive speed and waveform, as mutations in *flp-1* result in exaggerated movement, while overexpression causes sluggishness (Li et al., 1999). In addition, *flp-1* and *flp-18* are crucial for balancing excitation and inhibition in the locomotory circuit (Stawicki et al., 2013). While *C. elegans* shows complex locomotive behaviors, including forward and backward crawling, swimming, stomatal oscillation, head lifts, and omega turns (CROLL, 1975; Gray et al., 2005; Pierce-Shimomura et al., 2008), the contribution of *flp* genes to these specific locomotive behaviors have not been fully explored.

Here, we investigate the functional role of the SMB neurons in regulating various locomotive behaviors, including stomatal oscillation, reversal, head lifts, and omega turn. *lim-4* mutant animals which are defective in SMB development, show defects in both head locomotion and body locomotion. Defects in neuropeptide signaling result in abnormalities in stomatal oscillation, head lifts, and reversals, but not in omega turns. The FMRFamide-related peptide, *flp-12* mutant animals, exhibit behavioral defects such as stomatal oscillation, head lifts, omega turns, and reversals, similar to those observed in *lim-4* mutants. These defects can be restored by expressing *flp-12* cDNA under the control of the SMB-specific promoter. Moreover, RNAi

screening of FRPR families reveals that *frpr-8* mutant animals exhibit defects in stomatal oscillation similar to those observed in *flp-12* mutants. The *frpr-8* gene is expressed and acts in the AVD interneurons to mediate stomatal oscillation. Furthermore, heterologous expression of FRPR-8 using *Xenopus* oocytes or HEK293T cells conferred responsiveness to FLP-12. Together, these results reveal that FLP-12 neuropeptide secreted from the SMB neurons acts in the AVD neurons through FRPR-8 receptor to mediate stomatal oscillation.

## RESULTS

### The SMB neurons regulate the head and body locomotion of *C. elegans*

*lim-4* encodes a LIM homeodomain protein that specifies AWB and ADF chemosensory and SMB motor neuron identity (Dawid et al., 1995; Kim et al., 2015; Sagasti et al., 1999; Zheng et al., 2005). *lim-4* mutants have been shown to move in a coiled or loopy pattern (Sagasti et al., 1999), mainly due to a functional defect in the SMB motor neurons (Kim et al., 2015) (Fig. 1B). To further investigate the function of the SMB neurons, we measured the wavelength and wave width of wild-type and *lim-4* mutant animals. Consistent with previous reports, we found that *lim-4* mutants showed a significantly emphasized waveform (wild-type; wavelength: 489.730 μm ± 7.781, wave width: 123.185 μm ± 5.445, n=30, *lim-4*; wavelength: 569.436 μm ± 18.370, wave width: 264.067 μm ± 17.252, n=30; Fig. 1B).

Since the SMB neurons innervate the head and neck muscles (Fig. 1A) (McIntire et al., 1993; Sagasti et al., 1999), we examined the additional contributions of the SMB neurons to head and body locomotion, including stomatal oscillation, head lift, reversal, and omega turn (Fig. 1C) (CROLL, 1975). Stomatal oscillation refers to the worm's gentle movement of its head from side to side on the plate in the absence of food (Fig. 1C) (CROLL, 1975). Head lift indicates the movement of a worm raising its head above the surface of the plate (Fig. 1C) (CROLL, 1975) .We found that *lim-4* mutants showed increased stomatal oscillation, head lifts, and omega turn, but decreased reversals (for 3 minutes: wild-type; stomatal oscillation: 24.488 ± 1.545, head lifts: 5.186 ± 0.672, reversals: 6.907 ± 0.459, omega turn: 2.698 ± 0.351, n = *86, lim-4*; stomatal oscillation: 47.067 ± 3.152, head lifts: 21.933 ± 3.126, reversals: 3.867 ± 0.819, omega turn: 11.067 ± 1.667, n = 30; Fig. 1D).

To further investigate whether the SMB neurons directly regulate these head and body locomotive behaviors, we optogenetically stimulated the SMB neurons by expressing red-shifted channelrhodopsin (ReaChR) under the control of the *flp-12Δ3* promoter, which is specifically expressed in the SMB neurons (Fig. 1E) (Kim et al., 2015; Lin et al., 2013). We found that optogenetic activation of the SMB neurons did not elicit acute responses but resulted in decreased stomatal oscillation, while head lift, reversal, and omega turn were not altered (Fig. 1F, Supplementary Fig. S1). Together, these results indicate that the SMB neurons may play an indirect and chronic role in regulating head and body locomotor activities in *C. elegans*.

**Neuropeptidergic signaling in the SMB neurons mediates the head and body locomotion of *C. elegans***

Previous studies have shown that the SMB neurons exhibit both cholinergic and peptidergic features (Duerr et al., 2008; Kim et al., 2015; Kim and Li, 2004). To determine whether the SMB neurons regulate head and body locomotion through neuropeptides, we expressed dsRNA of *unc-31* under the control of the SMB-specific promoter in wild-type animals (Fig. 2A). UNC-31 regulates $Ca^{2+}$ dependent exocytosis of dense-core vesicles in neuroendocrine cells (Speese et al., 2007). We found that SMB-specific knockdown of UNC-31 had little or weak effect on wavelength and wave width (Fig. 2B), indicating that these locomotive parameters may not be regulated by neuropeptides. However, we observed noticeable and dramatic changes in other tested locomotive behaviors in *unc-31* dsRNAi transgenic animals, in which stomatal oscillation and head lift were increased, whereas reversal was decreased, similar to *lim-4* mutants (Fig. 2C). Omega turns appeared to be weakly increased,

although not significantly different from wild-type worms (Fig. 2C) (SMBp::*unc-31*dsRNAi : stomatal oscillation: 46.633 ± 1.801, head lifts: 13.433 ± 1.957, reversal: 7.300 ± 0.818, omega turn: 5.233 ± 1.044, n = 30; wild-type: stomatal oscillation: 37.867 ± 1.501, head lifts: 6.067 ± 1.457, reversal: 10.900 ± 0.835, omega turn: 4.333 ± 0.448, n = 30; Fig. 2C). These results indicate that neuropeptide(s) from the SMB neurons regulate a subset of head and body locomotive parameters, especially stomatal oscillation and head lift.

**FMRFamide-related neuropeptide *flp-12* gene acts in the SMB neurons to regulate the head and body locomotion of *C. elegans***

To determine which neuropeptides are expressed in and act in the SMB neuron to mediate head locomotion, we searched *C. elegans* single-cell expression data generated by the CeNGEN consortium (Hammarlund et al., 2018) and found that *flp-12* is predominantly expressed in the SMB neurons (Supplementary Fig. S2A). *flp-12* encodes an FMRFamide-related neuropeptide (Kim and Li, 2004) (Fig. 2D). Previous studies have shown that transgenic animals expressing *flp-12*p::*gfp* transgene, which includes 2.6 kb of upstream sequence of the *flp-12* gene, are expressed in the SMB neurons (Kim et al., 2015; Kim and Li, 2004). We also generated the same *flp-12*p::*gfp* transgenic animals and recapitulated *flp-12* expression in the SMB neurons (Fig. 2E). To investigate the function of *flp-12*, we obtained the *flp-12* null mutant (*ok2409*), which has a deletion in the 2$^{nd}$ and 3$^{rd}$ exons of the *flp-12* gene and measured the parameters of head and body locomotion in *flp-12* mutants. We found that wavelength and width were not altered (Fig. 2F) in *flp-12* mutants. However, similar to SMB-specific *unc-31* dsRNAi transgenic animals, stomatal oscillation, head lifts, reversal and omega turn were significantly increased in

*flp-12* mutants (*flp-12*: wavelength: 463.494 μm ± 20.742, wave width: 146.988 μm ± 5.304, stomatal oscillation: 44.281 ± 2.507, head lifts: 12.500 ± 2.355, reversal: 11.313 ± 0.991, omega turn: 5.188 ± 0.584, n = 32; wild-type: wavelength: 452.774μm ± 21.773, wave width: 123.185μm ± 5.445, stomatal oscillation: 28.802 ± 1.073, head lifts: 5.186 ± 0.672, reversal: 6.907 ± 0.459, omega turn: 2.698 ± 0.351, n = 86; Fig. 2G). Thus, these results indicate that FLP-12 neuropeptides are expressed in the SMB neurons to mediate head and body locomotive behaviors.

**FRPR-8 GPCR regulates stomatal oscillation and omega turns**

We next sought to investigate which neuropeptide receptor(s) are coupled with FLP-12 to mediate head and body locomotion. In *C. elegans*, 149 putative neuropeptide receptors have been identified, although their exact functions are not fully understood (Beets et al., 2023; Ripoll-Sanchez et al., 2023). We began performing an RNA-mediated interference (RNAi) screen to search for neuropeptide genes whose knockdown exhibits the same or a similar stomatal oscillation phenotype to *flp-12* mutants. Among the 16 neuropeptide genes tested, we found that *frpr-8* RNAi or reduction of function caused an increase in stomatal oscillation similar to that in *flp-12* mutants but not in head lifts (Fig. 3A and Supplementary Fig. S3).

The *frpr-8* gene encodes an FMRFamide-like peptide seven-transmembrane G protein-coupled receptor (Fig. 3B). We obtained a deletion mutant allele (*tm10970*), in which a 197 bp deletion removes part of the 9$^{th}$ exon, causing a loss of 42 amino acids from the C-terminal end (Fig. 3B). We found that *frpr-8* deletion mutants recapitulated the *frpr-8* RNAi phenotype, showing increased stomatal oscillation (Fig. 3C). Moreover, in *frpr-8* deletion mutants, omega

turns were increased, whereas head lifts and reversals were not altered (Fig. 3C), indicating that FRPR-8 may be coupled to FLP-12 to mediate stomatal oscillation and omega turns, but not head lifts and reversals. We next generated *flp-12*; *frpr-8* double mutants and found that the stomatal oscillation and omega turn phenotype of *flp-12*; *frpr-8* double mutants were comparable to those of either the *flp-12* or *frpr-8* single mutants (Fig. 3C), supporting the idea that FRPR-8 is genetically coupled with FLP-12.

***frpr-8* is expressed in and acts in the AVD interneurons to regulate stomatal oscillation**

To investigate how FRPR-8 mediates stomatal oscillation, we examined the expression patterns of the *frpr-8* gene by generating transgenic animals expressing a reporter gene, in which a 2.1 kb promoter region of the *frpr-8* gene was fused to the mCherry fluorescent protein gene (Fig. 3D) and found that the *frpr-8* reporter gene was expressed in several head neurons (Fig. 3D). We also created transgenic animals (*frpr-8*p::*frpr-8* cDNA::*gfp*) expressing full-length GFP-tagged FRPR-8 proteins under the control of the *frpr-8* promoter and found that FRPR-8 proteins were localized in the plasma membranes of two types of head neurons (Fig. 3F). To identify which neurons express *frpr-8*, we crossed *frpr-8*p::*frpr-8* cDNA::*gfp* transgenic animals with NeuroPAL worms (Yemini et al., 2021) and observed colocalization of GFP with NeuroPAL signals in the AVD and SIA neurons (Figs. 3E, F), both of which are included in CeNGEN data (Hammarlund et al., 2018) (Supplementary Fig. S2B). Moreover, we further confirmed the *frpr-8* expression in the AVD neurons by colocalization with *nmr-1*p::*gfp* transgenic animals (Brockie et al., 2001) (Supplementary Fig. S4).

We next attempted to rescue the locomotive defects of *frpr-8* mutants by expressing wild-

type *frpr-8* cDNA under the control of its own *frpr-8* or the AVD-specific *nmr-1* promoters (Supplementary Fig. S4) (Ryu et al., 2018). Expression of FRPR-8 proteins in both the AVD and SIA neurons, as well as in the AVD neurons alone, was sufficient to restore locomotive phenotypes such as stomatal oscillation and omega turns in *frpr-8* mutants (Fig. 3G), indicating that *frpr-8* may act in the AVD neurons to regulate these locomotive behaviors. We also observed that overexpression of FRPR-8 in the AVD neurons increased head lifts (Fig. 3G), implying that FRPR-8 may play a role in regulating not only stomatal oscillation and omega turns but also head lifts.

**Optogenetic activation of the AVD interneurons increased stomatal oscillation**

While the SIA neurons regulate locomotive speed but not backward locomotion (Lee et al., 2019), the AVD interneurons have been shown to mediate backward locomotive behaviors, including reversals and omega turns. However, the contribution of the AVD neurons to head locomotion has not yet been explored. We generated transgenic animals expressing the channel rhodopsin variant ReaChR under the control of the *frpr-8* promoter. While the animals were allowed to move freely, light stimulation in the presence of all-trans-retinal (ATR) elicited an immediate increase in reversal and omega turns (Fig. 4A and Supplementary Figs. S5A and B), confirming that the AVD neurons regulate reversal and omega turns. We also observed that optogenetic activation of the AVD neurons increases stomatal oscillation but did not significantly increase head lift (Fig. 4A and Supplementary Figs. S5A and B). Although the SIA neurons can also contribute to stomatal oscillation, these data suggest that AVD neuronal activity regulates both backward behaviors and stomatal oscillation.

**GPA-7 G protein appears to be coupled with FRPR-8 to regulate stomatal oscillation**

The *C. elegans* genome encodes 21 G protein α-subunits (Jansen et al., 1999; Matúš and Prömel, 2018). Among these 21 Gα genes, *gpa-7* is predominantly expressed in the AVD neurons (Hammarlund et al., 2018). To confirm the expression of *gpa-7* in the AVD neurons, we generated transgenic animals expressing *gpa-7*p::*gfp* under the control of 3.1 kb promoter regions (Fig. 4B) and found that *gpa-7* is indeed co-expressed with *frpr-8* in the AVD neurons.

We then measured four locomotive parameters of the *gpa-7* mutant allele (*pk610*) (Fig. 4C) and found that *gpa-7* mutants exhibited an increase in stomatal oscillation similar to that of *frpr-8* mutants, while *gpa-7* mutants showed normal omega turns (Fig. 4C). These results indicate that *frp-8* may be coupled with *gpa-7* to mediate stomatal oscillation but not head lifts. Next, we created *gpa-7; frpr-8* double mutants, which showed stomatal oscillation comparable to either single mutant (Fig. 4C), suggesting that *frpr-8* and *gpa-7* act in the same pathway to regulate stomatal oscillation.

**FLP-12 neuropeptide activates the FRPR-8 GPCR *in vitro***

We next sought to investigate whether the FLP-12 neuropeptide is a ligand for the FRPR-8 GPCR using an *in vitro* cell expression system. We first expressed FRPR-8 in *Xenopus* oocytes with cRNA microinjection and performed two-electrode voltage-clamp experiments (Fig. 5A). When we administered 1 nM, 10 nM, 100 nM, and 1000 nM of FLP-12 to oocyte expressing FRPR-8 (Fig. 5B), and found that FLP-12 activated the FRPR-8 receptor (EC50 = 107.7 nM) in dose-dependent manner (Fig. 5B).

We also generated transgenic HEK293T cells that express FRPR-8 with the Gα16 subunit and used calcium indicator Fluo-4 to detect calcium elevation (Fig. 5A). We tested two cell lines, one that expresses FRPR-8 and one that does not. We treated them with 1 μM of FLP-12 for 1 minute, then measured the level of $Ca^{2+}$ in the cytosol of the cell. We observed that 1 μM of FLP-12 induced $Ca^{2+}$ elevation in cells expressing FRPR-8 but not in cells transfected with empty vector (Fig. 5C). As a control, we treated the transgenic cells with FLP-5, which has the same length as FLP-12 but only shares FMRF sequence in C-terminus (Fig. 5D). Unlike FLP-12, FLP-5 exposure did not elicit $Ca^{2+}$ elevation, indicating that FLP-12 activates FRPR-8. These data indicate that FLP-12 neuropeptide indeed interacts with FRPR-8 GPCR.

## DISCUSSION

*Caenorhabditis elegans* exhibits diverse locomotive behaviors such as crawling, swimming, reversal, omega turn, stomatal oscillation, and head lift, which are modulated by external conditions and internal states and serve as a simple model to understand more complicated locomotion of higher animals (Moon et al., 2021; Park et al., 2022). Recent studies have shown the importance of FLP neuropeptide signaling in understanding locomotive behaviors. For example, FMRFamide related peptide FLP-20 functions through FRPR-3 GPCR to regulate speed during arousal in response to mechanosensory stimuli, and FLP-2 modulates locomotion via FRPR-18 GPCR (Chen et al., 2016; Chew et al., 2018). FLP-11, FLP-24, and FLP-13 regulate the stopping of locomotion during quiescence and sleep (Nath et al., 2016; Turek et al., 2016). FLP-8, FLP-19, FLP-12, and FLP-20 regulate turning during mating (Liu et al., 2007). Here, we further identify a function of FLP-12 in the stomatal oscillation through

FRPR-8 GPCR and GPA-7 G proteins.

The SMB head motor neurons have unbranched and synapse-free processes along the body and innervate head and body muscles (White et al., 1986). Previous studies have shown that the SMB neurons control the wavelength and width of their body undulations (Kim et al., 2015). More recently, Matsumoto et al. (PNAS, 2024) showed that SMBD plays a crucial role in integrating sensory and motor information to regulate klinotaxis in *C. elegans*, with SMBD responding to temporal changes in NaCl concentration and exhibiting activity closely correlated with neck bending. Here, we provide multiple lines of evidence showing that the SMB neurons regulate other head and body locomotion through the action of neuropeptides. First, chronic optogenetic activation of the SMB neurons exhibited decreased stomatal oscillation. Second, RNAi of the dense core vesicle gene *unc-31* in the SMB neurons caused head/body locomotion defects. Third, deletion mutation of the SMB-expressed *flp-12* (FMRFamide-like neuropeptide) gene caused defects in head and body locomotion, but not in wavelength or width. Lastly, the SMB-specific *flp-12* cDNA expression restored the head and body locomotion defects of *flp-12* mutants. Together, we conclude that the SMB neurons suppress head and body locomotion through FLP-12 neuropeptide.

Based on our results, we propose a model in which FLP-12 neuropeptide regulates stomatal oscillation through its interaction with the FRPR-8 GPCR and the GPA-7 G protein (Fig. 6). Once released from the SMB neurons, FLP-12 binds to the FRPR-8 receptor on the AVD neurons, which serve as command interneurons orchestrating complex motor outputs. Activation of FRPR-8 by FLP-12 was validated both *in vitro* and *in vivo*. *In vitro* experiments showed that FLP-12 induces a dose-dependent activation of FRPR-8 in *Xenopus* oocytes. *In vivo*,

genetic knockdown and mutant studies revealed that the loss of FRPR-8 results in behavioral changes similar to those observed in *flp-12* mutants, including increased stomatal oscillation. Moreover, GPA-7, a G protein α-subunit expressed in the AVD neurons, is implicated as a downstream effector of FRPR-8. Mutants lacking GPA-7 exhibit an increase in stomatal oscillation, similar to the phenotype seen in FRPR-8 mutants. This suggests that FRPR-8 activation by FLP-12 in AVD neurons triggers a signaling cascade involving GPA-7, which modulates the execution of stomatal oscillation (Fig. 6). Thus, this neuropeptidergic circuit highlights the role of the SMB-AVD neuropeptide network as critical nodes in translating sensory inputs into coordinated motor outputs, particularly in behaviors related to stomatal oscillation.



## MATERIALS and METHODS

### Strains

All strains were maintained at 20°C (Brenner, 1974). The N2 Bristol strain was used as a wild-type strain. All the mutants and transgenic strains used in this study are listed in S1 Table.

### Molecular biology and transgenic worms

All the constructs derived in this study were inserted into the pPD95.77 vector (Fire et al., 1990). For the *flp-12*, *frpr-8*, and *gpa-7* promoter expression, 2.6 kb, 2.1 kb, and 3.1 kb promoter regions were amplified by PCR from N2 genomic DNA and used to generate *flp-12*p::*gfp*, *frpr-*

*8*p::*gfp*, *frpr-8*p::*mCherry*, and *gpa-7*p::*gfp*. *nmr-1*p::*gfp* and *nmr-1*p::*GCaMP* transgenic animal was used in previous study (Ryu et al., 2018). To generate transgenic worms, 50 ng of *flp-12*p::*gfp*, and *gpa-7*p::*gfp* construct was injected, with 50 ng of *unc-122*p::*dsRed* as an injection marker. To generate *frpr-8* promoter transgenic animals, 150 ng *frpr-8*p::*gfp* and *frpr-8*p::*mCherry* construct was injected, with 50ng of *unc-122*p::*dsRed* (Heo et al., 2023). For the rescue experiments, the *flp-12* cDNA was amplified by PCR from a cDNA library. The *frpr-8 cDNA* was synthesized by MACROGEN. With 50 ng of *unc-122*p::*gfp* as an injection marker, 50 ng of the *flp-12* cDNA under the control of *flp-12* promoter was injected into *flp-12* mutants. With 50 ng of *frpr-8* cDNA under the control of *nmr-1* and *frpr-8* promoters were injected into *frpr-8* mutants. Forward and reverse primer for *unc-31* dsRNA was searched at E-RNAi service from German cancer research center (dkfz.de). *unc-31* dsRNA was amplified by PCR from a cDNA library and fused with the *flp-12* promoter. 50 ng of fused *flp-12*p::*unc-31*dsRNA was injected into wild-type with 50 ng of *unc-122*p::*dsRed* as an injection marker. For heterologous expression, *frpr-8* cDNA was subcloned to pcDNA3.1 construct.

**Head locomotive behavior tracking and phenotype analysis**

To record animal locomotion, NGM agar plates were used. Well-fed young adult hermaphrodite worms were used to record under a Leica High-performance Fluorescence Stereomicroscope (M205FA) using the Leica Application Suite 4.2 software. To quantify the locomotory behaviors, worms were transferred from a seeded NGM plate to a non-seeded plate. After 30 seconds of acclimation, video recording was conducted for 3 minutes. Each type of head and body locomotory behavior was quantified as follows (CROLL, 1975). Stomatal Oscillation was

characterized by rapid side-to-side head movements during turning, forward, or backward locomotion, and was confined to the anteriormost 10-15 μm of the worm. A head lift was recorded when the worm raised its head off the substrate, involving up to 50-70 μm of the anterior region. Reversal was defined as the initiation of backward movement starting from the anterior, propagating through the entire body. The backward movement includes undulatory waves, typically producing approximately 1.5 waves per body length. An omega turn was counted when the worm makes a pronounced lateral movement, continuing until the head touches or nearly touches the tail.

**RNAi assay**

RNAi was induced by feeding as described (Timmons et al., 2001). Ahringer lab RNAi library was used for RNAi assay. NR350 strain was used for assay and cultivated at 20℃. The following RNAi clones were used to feed: L4440 empty vector control, *frpr-1* (clone C02B8.5), *frpr-2* (clone C05E7.4), *frpr-3* (clone C26F1.6), *frpr-4* (clone C54A12.2), *frpr-5* (clone C56A3.3), *frpr-8* (clone F53A9.5), *frpr-12* (clone K06C4.9), *frpr-14* (clone K07E8.5), *frpr-15* (clone K10C8.2), *frpr-16* (clone R12C12.3), *frpr-17* (clone T14C1.1), *frpr-18* (clone T19F4.1), *frpr-19* (clone Y41D4A.8), clone C09F12.3, clone D1014.2, *npr-13* (clone ZC412.1).

**Recording of *Xenopus* oocytes by two electrode voltage clamping (TEVC)**

TEVC was performed as described previously (Du and Kang, 2020). Briefly, oocyte-positive *Xenopus* females were obtained from Korea Xenopus resource center for research

(http://kxrcr.knrrc.or.kr/). Surgically removed ovaries were incubated with 1.5 mg/ml collagenase (type II, LS004196, Worthington, NJ, USA) for 1.5 hrs with gentle rocking. The remaining follicular layer was manually peeled off from oocytes before capped RNA (cRNA) microinjection. For expression of FRPR-8, cRNA was in vitro transcribed with T3 promoter with the use of mMessage mMachine T3 transcription kit (Invitrogen, CA, USA). For control cells, water was microinjected. Approximately 20 hrs at 18℃ after microinjection, the oocytes were subjected to TEVC recording. FLP-12 was perfused in nominally calcium-free recording solution (100 NaCl, 1 KCl, 1 MgCl2, 5 HEPES, pH 7.6) at 1, 10, 100 and 1,000 nM. Voltage was initially held at -60 mV and ramped to +60 mV for 300 ms every second. The current was recorded at 2,000 Hz by the GeneClamp 500B amplifier (Molecular Devices, CA, USA) and subjected to data acquisition (Digidata 1440A, Molecular Devices, CA, USA). Peak current data at each concentration were used to generate a dose dependence curve. The dose dependence was fitted to Hille equation using Sigmaplot14.0.

**Cell culture**

HEK293T cells were maintained in Dulbecco Modified Eagle Medium (DMEM, Invitrogen, CA) supplemented with 10% Fetal Bovine Serum (FBS, Invitrogen, CA) and 0.2% penicillin/streptomycin (Invitrogen, CA) in 100-mm culture dishes at 37°C with 5% $CO_2$. For transfection, Lipofectamine 2000 (Invitrogen, CA) was used when the confluency of cells reached 50–70%. cells were co-transfected with FRPR-8 and Gα16. Transfected cells were plated onto coverslip chip coated with poly-L-lysine (0.1 mg/ml, Sigma-Aldrich, MO) 24 to 36 h after transfection. Plated cells were used for confocal experiments within 24 h after plating.

**Confocal imaging**

All imaging was performed with an LSM 700 confocal microscope (Carl Zeiss AG) at room temperature (22-25℃). The Ringer's solution for confocal imaging contained 160 mM NaCl, 2.5 mM KCl, 2 mM CaCl2, 1 mM MgCl2, 10 mM HEPES, and 8 mM glucose, adjusted to pH 7.4 with NaOH and osmolarity of 321 to 350 mOsm. Fluo4-AM (Invitrogen) was prepared as 1 mM stocks in DMSO and diluted to 1:250 in Ringer's solution. For time courses, images were obtained by scanning cells with a 40x (water) apochromatic objective lens at 512 x 512 pixels using digital zoom. To analyze the time courses of the degree of cytosolic fluorescence of Fluo4-AM, images were taken every 3s in Zeiss ZEN imaging software. Regions of interest were selected in the cytosolic regions of cells, and quantitative analysis was performed using the ZEN 2012 imaging software (Carl Zeiss MicroImaging). All confocal images were transferred from TIFF formats, and raw data from the time course were processed with Microsoft Office Excel 2016 and summarized in Igor Pro (WaveMetrics Inc.).

**Neuronal Cell ID**

Cell identification was done by assessing position and size using Nomarski optics and by crossing with NeuroPAL (*otIs699*, *otIs670*) (Yemini et al., 2021). Imaging experiments using the NeuroPAL line were conducted using a Zeiss LSM780 laser-scanning confocal, with settings available for download on yeminilab.com. Analysis of NeuroPAL images for cell identification was conducted as in Yemini et al. (2021).

**Optogenetics**

For activating the SMB head motor neurons and the AVD neurons, L4 transgenic worms expressing ReaChR::mKate2 under the control of *flp-12* and *frpr-8* promoters were used. Transgenic strains were transferred 12 hr before the assay to NGM plates seeded with *E.coli* OP50 plates or *E.coli* OP50-retinal containing 1 mM all-trans-retinal (ATR, Sigma). The assays were performed in the 60 mm diameter NGM plates without *E.coli* OP50. To activate ReaChR, 565 nm LED at roughly 0.1 mW/square mm was used (LED light source, Thorlabs). Optogenetic experiments were recorded using a Leica High-performance Fluorescence Stereomicroscope (M205FA) for 3 min, with the light stimulus being exposed 1 min after the start of the video recording. Each behavior was counted manually using image J software.



**ACKNOWLEDGMENTS**

We are grateful to the *Caenorhabditis* Genetics Center (NIH Office of Research Infrastructure Programs, P40 OD010440) and the National BioResource Project (Japan) for strains. We are also grateful to Chris Li, and K. Kim Labs for helpful discussion and/or critical comments on this manuscript. This work was supported by the National Research Foundation of Korea ((RS-2024-00356180 to KH.Kim), the DGIST International Joint Research Project (24-KUJoint-07 to KH.Kim), the Korea Brain Research Institute (23-BR-01-02, 22-BR-03-06 to KJ.

Kang), Korea Food Research Institute (E0210101 to J. Hahm), and the National Research Foundation of Korea (2022R1A2C1006560, RS-2024-00351000 to B.C. Suh).

## AUTHOR CONTRIBUTIONS

D.K., K.M. M., W. H., E.J.D., C. P., and J. C., performed the experiments; J. H. provides reagents; B. S., KJ. K., and KH.K. analyzed and interpreted data; and D.K., K.M. M., W. H., and KH.K. wrote the manuscript.

## CONFLICT OF INTEREST

Authors do not have any competing financial interests.

## FIGURE LEGENDS

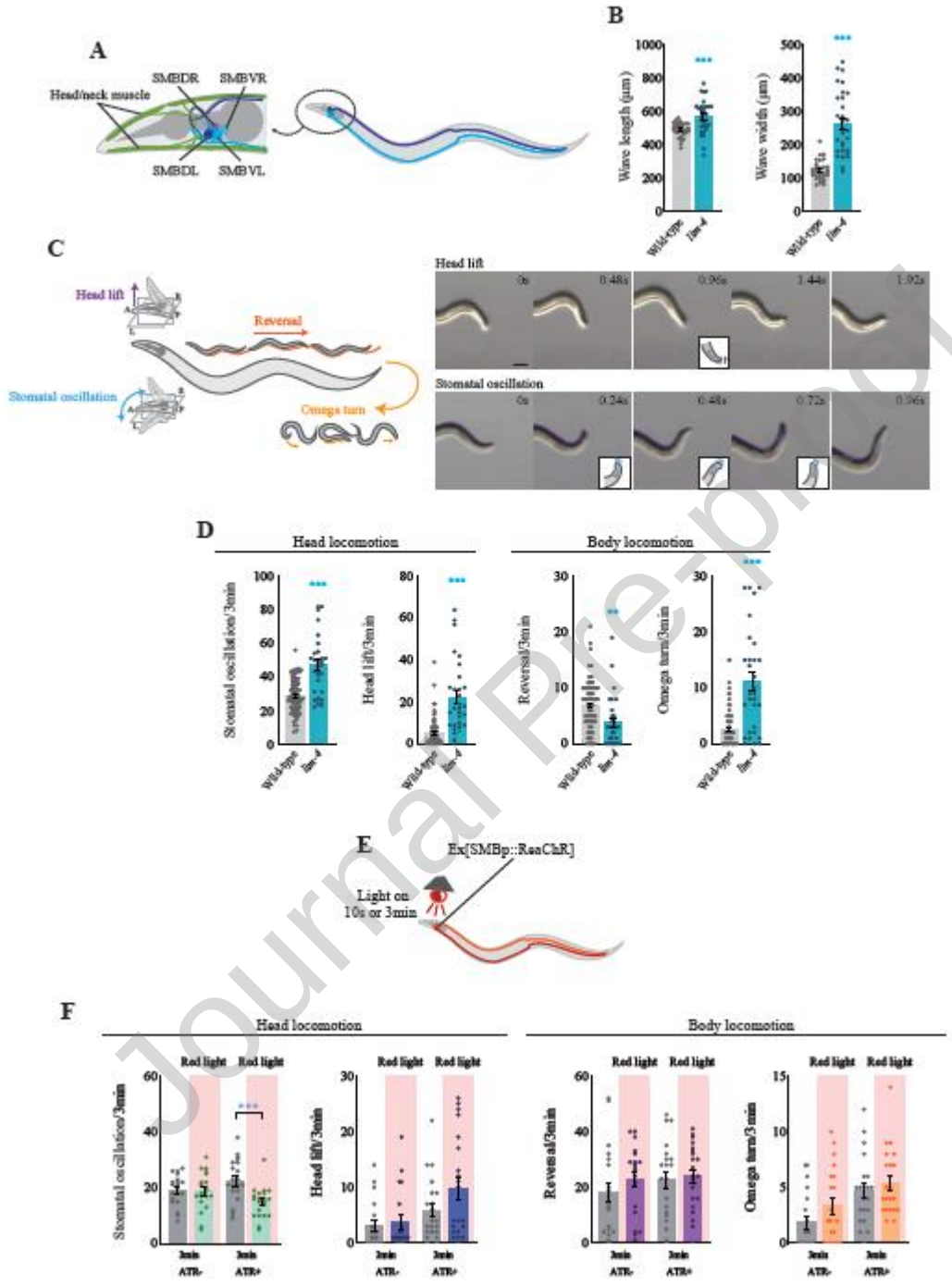


Figure 1. The SMB neurons regulate head and body locomotion

(A) Scheme of the SMB sensory/inter/motor neurons. (B) Wavelength and wave width of wild-type and *lim-4* mutant. n = 30. (C) Scheme of head lift, stomatal oscillation, reversal, and omega turn (left) and time lapse images during head lift and stomatal oscillation (right). (D) The frequency of stomatal oscillation, head lift, reversal, and omega turn behavior of wild-type and *lim-4* mutant for 3 minutes. n = 30 ~ 86. (E) Scheme of the optogenetic activation of the SMB neurons. (F) The frequency of stomatal oscillation, head lift, reversal, and omega turn behavior of wild-type animals upon optogenetic activation of the SMB neurons. Light stimulation was performed in the absence or presence of all-trans-retinal (ATR) for 3 minutes. n = 20. Error bars represent the SEM. *, **, and *** indicate a significant difference from the control at $p<0.05$, 0.01, and 0.001 by a student t-test, respectively.

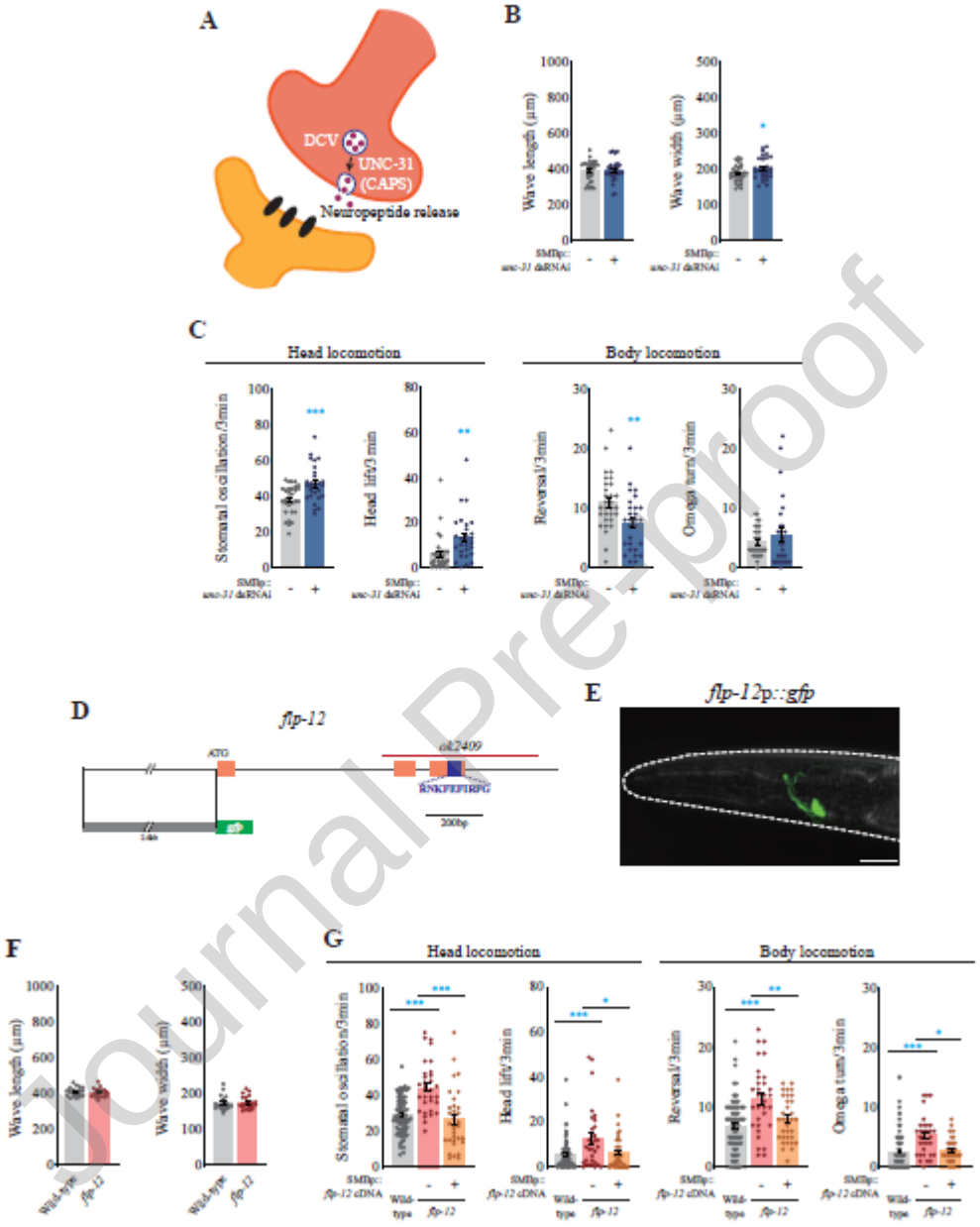


Figure 2. FLP-12 neuropeptide expressed in the SMB neurons regulates head and body locomotion

(A) Schematic of UNC-31 function in neurons. (B) Wavelength and wave width of wild-type and

transgenic animals expressing SMB(*flp-12*)p*::unc-31* dsRNAi. n = 30. (C) The frequency of head and body locomotive behaviors of wild-type and transgenic animals expressing SMBp*::unc-31* dsRNAi for 3 minutes. n = 30. (D) The genomic structure of the *flp-12* gene. (E) Expression pattern of *flp-12*p::*gfp*. The anterior is to the left. Scale bar: 20 μm. (F) Wavelength and wave width of wild-type and *flp-12* mutant animals. n = 30. Error bars represent the SEM. *, **, and *** indicate a significant difference from the control at $p<0.05$, 0.01, and 0.001 by a student t-test, respectively. (G) The frequency of head and body locomotive behaviors of wild-type, *flp-12* mutant, and *flp-12* mutant expressing *flp-12* cDNA under the control of SMB-specific (*flp-12*) promoter for 3 minutes. n = 30 ~ 86. Error bars are the SEM. *, **, and *** indicate significantly different from the wild-type at $p<0.05$, 0.01, and 0.001 by a one-way ANOVA with a Tukey post hoc test, respectively.

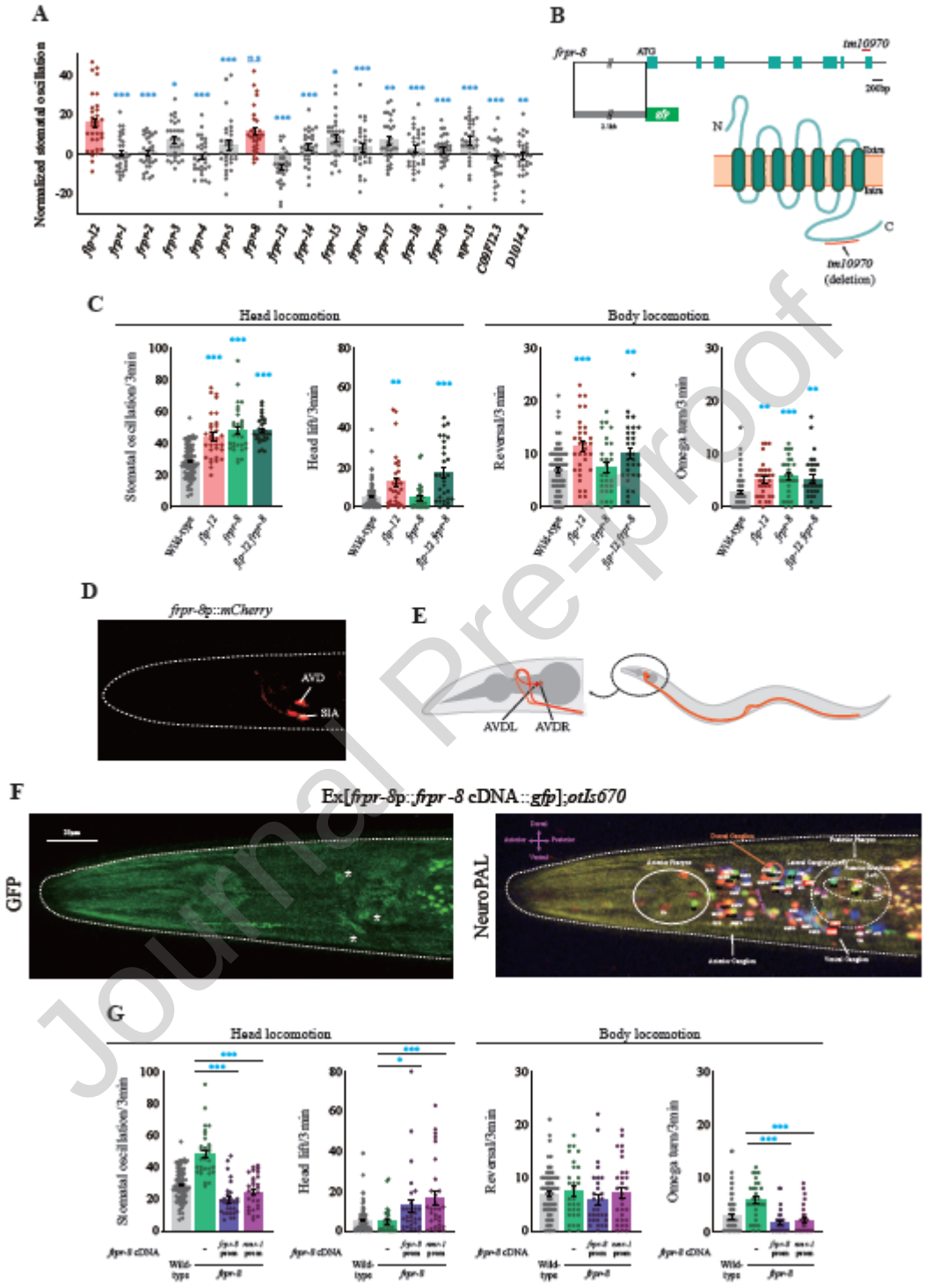


Figure 3. FRPR-8 GPCR is expressed in and acts in the AVD neurons to mediate FLP-12

mediated stomatal oscillation

(A) The frequency of normalized stomatal oscillation of *flp-12* mutants and RNAi-treated worms against neuropeptide candidate receptors for 3 minutes. n = 30 ~ 32. Error bars are the SEM. *, **, and *** indicate significantly different from the wild-type at $p<0.05$, 0.01, and 0.001 by a one-way ANOVA with a Dunnett post hoc test, respectively. (B) The genomic structure of the *frpr-8* gene. (C) The frequency of stomatal oscillation, head lift, reversal, and omega turn behavior of wild-type, *flp-12*, *frpr-8*, and *flp-12 frpr-8* double mutants for 3 minutes. n = 30 ~ 86. (D) Representative image of wild-type expressing the *frpr-8*p::*mCherry* transgene in the AVD neurons. Anterior is to the left. Scale bar: 20 μm. (E) Schematic drawing of the AVD neurons in *C. elegans*. (F) Representative images of NeuroPAL *otIs670* worm expressing *frpr-8*p::*frpr-8* cDNA::*gfp*. Left and right images represent GFP-tagged *frpr-8* cDNA and NeuroPAL images, respectively. Images are derived from z-stacks of confocal microscopy images. The anterior is to the left. Scale bar: 20 μm. (G) The frequency of stomatal oscillation, head lift, reversal, and omega turn behavior of wild-type, *frpr-8*, and transgenic animals expressing *frpr-8* cDNA under the control of *frpr-8* or *nmr-1* promoters for 3 minutes. n = 30 ~ 86. Error bars are the SEM. *, **, and *** indicate significantly different from the wild-type at $p<0.05$, 0.01, and 0.001 by a one-way ANOVA with a Tukey post hoc test, respectively.

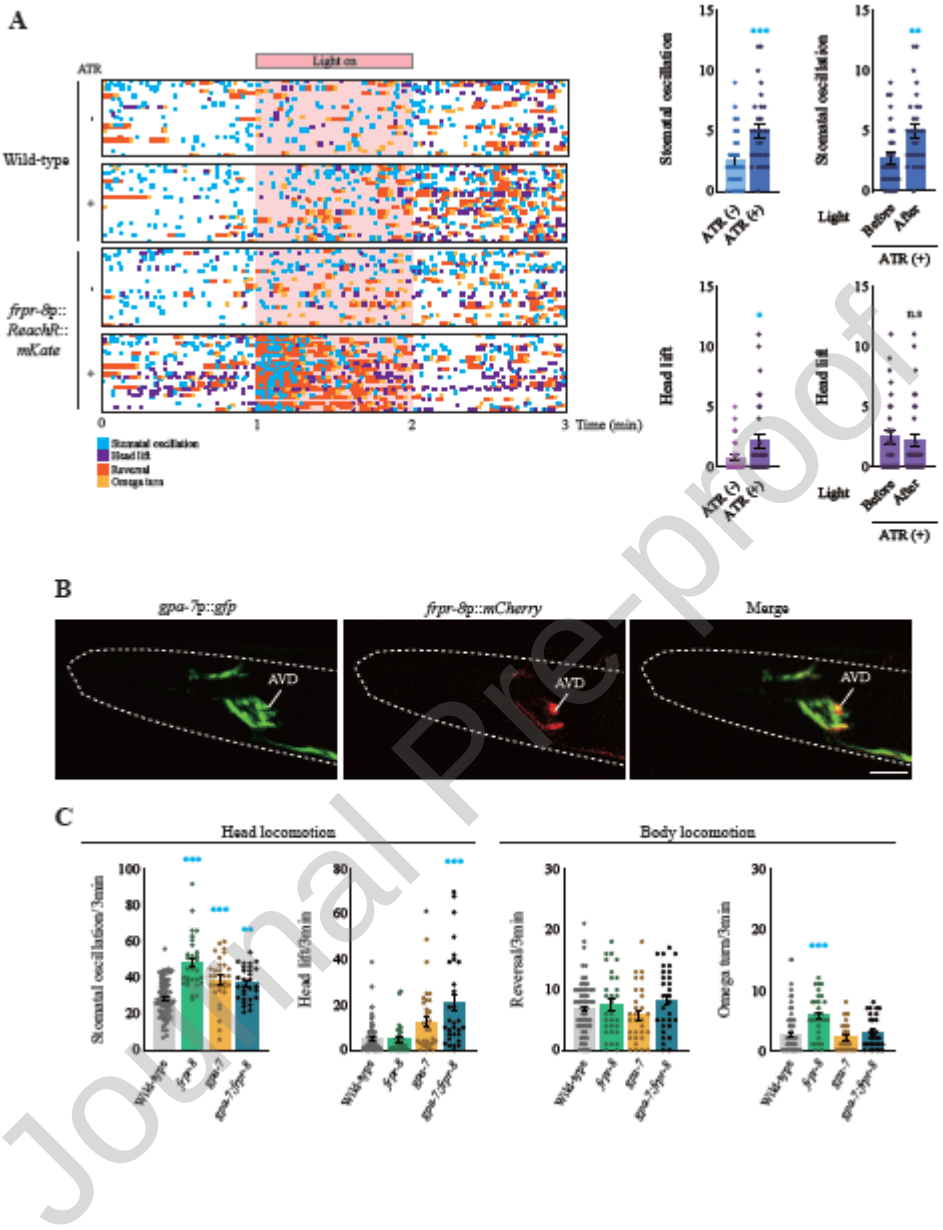


Figure 4. Gα subunit protein *gpa-7* is coupled to *frpr-8* GPCR to regulate stomatal oscillation

(A) Timescale images of optogenetics activation of the AVD neuron (left panel). The frequency of stomatal oscillation (right upper) and head lift (right lower). n = 30. Error bars represent the SEM. *, **, and *** indicate a significant difference from the control at $p<0.05$, 0.01, and 0.001

by a student t-test, respectively. (B) Expression pattern of transgenic animals expressing *gpa-7*p::*gfp* (left) and *frpr-8*p::*mCherry* transgene (middle). Merged images are in the right panel. Images are derived from z-stacks of confocal microscopy images. The anterior is to the left. Scale bar: 20 μm. (C) The frequency of stomatal oscillation, head lift, reversal, and omega turn behavior of wild-type, *frpr-8*, *gpa-7*, and *gpa-7; frpr-8* double mutants for 3 minutes. n = 30 ~ 86. Error bars are the SEM. *, **, and *** indicate significant differences from the wild-type at $p<0.05$, 0.01, and 0.001 by a one-way ANOVA with a Tukey post hoc test, respectively.

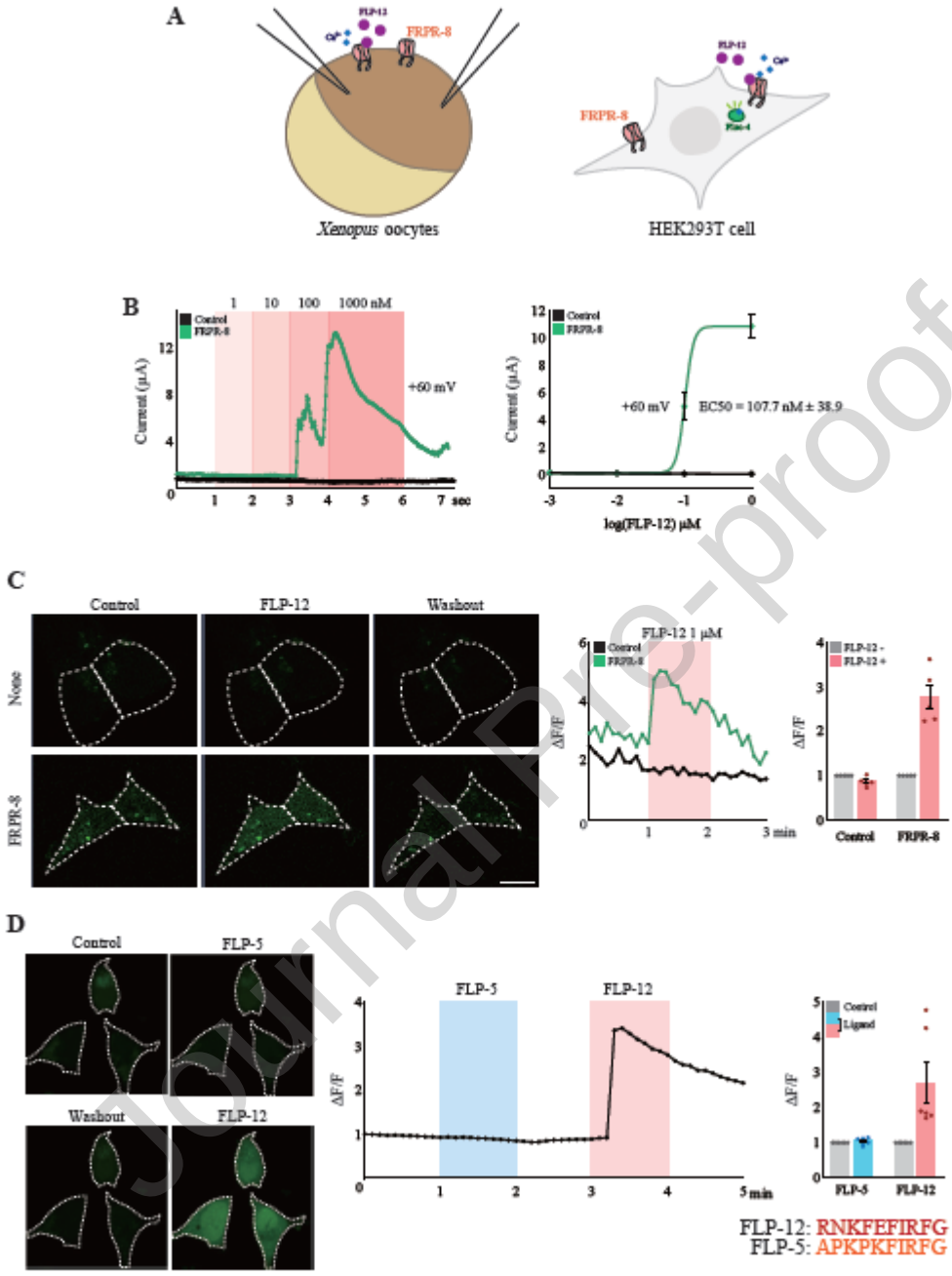


Figure 5. FLP-12 is a cognate ligand of FRPR-8

(A) Schematic images of two distinct *in vitro* systems, *Xenopus* oocyte (left) and HEK293T cell

(right). (B) A representative current trace (Left) at +60 mV from *Xenopus* oocytes microinjected with either FRPR-8 cRNA (green) or water (control, black). The experiments were then plotted to present FLP-12 dose dependence of the cells (Right). (C) Time-series confocal images of HEK293T cells (left), which are expressed without or with FRPR-8, were taken before (left), during 1 μM FLP-12 treatment (middle), and after washout (right). All cells expressed Gα and calcium indicator Fluo-4, which was used to detect the calcium elevation. Scale bar: 10 μm. Representative time courses of cytosolic fluorescence intensity change in HEK293T cells in response to FLP-12 treatment. Lines indicate the activity of the cells without (black) or with (green) FRPR-8. Fluorescence intensity changes (right). Gray bars indicate before treatment of FLP-12, and red bars indicate after treatment of FLP-12 neuropeptide. $n \geq 5$. Error bars are the SEM. (D) Time-series images and fluorescence intensity change of FRPR-8 expressed cells with FLP-5 or FLP-12 treatment. Time-series confocal images of HEK293T cells expressing FRPR-8 were taken before (control), during FLP-5 (1 μM) treatment, washout, and FLP-12 (1 μM) treatment (left). Representative time courses of cytosolic fluorescence intensity changes in cells in response to FLP-5 and FLP-12. Fluorescence intensity changes (right). Gray bars indicate before the treatment of ligands, and colored bars indicate after the treatment of ligands. $n \geq 5$. Error bars indicate SEM.

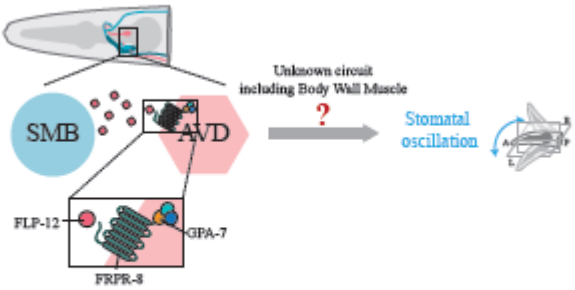


Figure 6. Model of FLP-12 and FRPR-8 regulating stomatal oscillation



**SUPPLEMENTARY FIGURE LEGENDS**

Supplementary Figure 1. Optogenetic activation of the SMB neurons showed increased omega turn but not in head lifts and reversal

The frequency of head lifts, reversal and omega turn in no light for 10 seconds, red light (red box) for 10 seconds, and no light for 10 seconds. n = 20. Error bars are the SEM. *, **, and *** indicate significant differences from the wild-type at $p<0.05$, 0.01, and 0.001 by a one-way ANOVA with a Tukey post hoc test, respectively.

Supplementary Figure 2. CeNGEN RNA expression data

(A) Candidate neuropeptides which are expressed in the SMB neurons. (B) *frpr-8* expressed neurons.

Supplementary Figure 3. RNAi screening to find *flp-12* neuropeptide receptor genes.
The frequency of normalized head lifts of *flp-12* mutants and RNAi-treated worms against neuropeptide candidate receptors for 3 minutes. n = 30 ~ 32. Error bars are the SEM. *, **, and *** indicate significant differences from the wild-type at $p<0.05$, 0.01, and 0.001 by a one-way ANOVA with a Dunnett post hoc test, respectively.

Supplementary Figure 4. *frpr-8* is expressed in the AVD neurons
Images (upper) of adult transgenic animals expressing *frpr-8*p::*mCherry* (left) that also express *nmr-1*p::*gfp* transgene (middle). Merged images are in the right panel. Images are derived from z-stacks of confocal microscopy images. The anterior is to the left. Scale bar: 20 μm. Images (bottom) of transgenic animals expressing GFP-tagged *frpr-8* cDNA driven under the control of *frpr-8* promoter. Images in the boxed regions are single-focal-plane confocal microscopy images of the AVDR and AVDL cell bodies. The upper side is to the head. Scale bar: 20 μm.

Supplementary Figure 5. Optogenetic activation of the AVD neurons showed an increased reversal and omega turn
(A) The frequency of reversal and omega turn in the optogenetic activation of the AVD neurons. n = 30. Error bars represent the SEM. *, and *** indicate a significant difference from the control at $p<0.05$, and 0.001 by a student t-test, respectively. (B) The frequency of stomatal oscillation, head life, reversal and omega turn in no light for 1 minute, red light (red box) for 1 minute, and no light for 1 minute. n = 30. Error bars are the SEM. *, **, and *** indicate significant differences from the wild-type at $p<0.05$, 0.01, and 0.001 by a one-way ANOVA with

a Tukey post hoc test, respectively.

## REFERENCES

Beets, I., Zels, S., Vandewyer, E., Demeulemeester, J., Caers, J., Baytemur, E., Courtney, A., Golinelli, L., Hasakiogullari, I., Schafer, W.R., et al. (2023). System-wide mapping of peptide-GPCR interactions in C. elegans. Cell Rep 42, 113058.

Bhat, U.S., Shahi, N., Surendran, S., and Babu, K. (2021). Neuropeptides and Behaviors: How Small Peptides Regulate Nervous System Function and Behavioral Outputs. Front Mol Neurosci 14, 786471.

Brenner, S. (1974). The genetics of Caenorhabditis elegans. Genetics 77, 71-94.

Brockie, P.J., Mellem, J.E., Hills, T., Madsen, D.M., and Maricq, A.V. (2001). The C. elegans glutamate receptor subunit NMR-1 is required for slow NMDA-activated currents that regulate reversal frequency during locomotion. Neuron 31, 617-630.

Chen, D., Taylor, K.P., Hall, Q., and Kaplan, J.M. (2016). The Neuropeptides FLP-2 and PDF-1 Act in Concert To Arouse Caenorhabditis elegans Locomotion. Genetics 204, 1151-1159.

Chew, Y.L., Tanizawa, Y., Cho, Y., Zhao, B., Yu, A.J., Ardiel, E.L., Rabinowitch, I., Bai, J., Rankin, C.H., Lu, H., et al. (2018). An Afferent Neuropeptide System Transmits Mechanosensory Signals Triggering Sensitization and Arousal in C. elegans. Neuron 99, 1233-1246 e1236.

CROLL, N.A. (1975). Components and patterns in the behaviour of the nematode Caenorhabditis elegans. Journal of Zoology 176, 159-176.

Dawid, I.B., Toyama, R., and Taira, M. (1995). LIM domain proteins. C R Acad Sci III 318, 295-306.

Du, E.J. and Kang, K. (2020). A Single Natural Variation Determines Cytosolic Ca(2+)-Mediated Hyperthermosensitivity of TRPA1s from Rattlesnakes and Boas. Mol Cells 43, 572-580.

Duerr, J.S., Han, H.P., Fields, S.D., and Rand, J.B. (2008). Identification of major classes of cholinergic neurons in the nematode Caenorhabditis elegans. J Comp Neurol 506, 398-408.

Fire, A., Harrison, S.W., and Dixon, D. (1990). A modular set of lacZ fusion vectors for studying gene expression in Caenorhabditis elegans. Gene 93, 189-198.

Froemke, R.C. and Young, L.J. (2021). Oxytocin, Neural Plasticity, and Social Behavior. Annual Review of Neuroscience, Vol 44, 2021 44, 359-381.

Gray, J.M., Hill, J.J., and Bargmann, C.I. (2005). A circuit for navigation in Caenorhabditis elegans. Proc Natl Acad Sci U S A 102, 3184-3191.

Hammarlund, M., Hobert, O., Miller, D.M., 3rd, and Sestan, N. (2018). The CeNGEN Project: The Complete Gene Expression Map of an Entire Nervous System. Neuron 99, 430-433.

Heo, W., Hwang, H., Kim, J., Oh, S.H., Yu, Y., Lee, J.H., and Kim, K. (2023). The CCAAT-box transcription factor, NF-Y complex, mediates the specification of the IL1 neurons in C. elegans. BMB Rep 56, 153-159.

Jansen, G., Thijssen, K.L., Werner, P., van der Horst, M., Hazendonk, E., and Plasterk, R.H. (1999). The complete family of genes encoding G proteins of Caenorhabditis elegans. Nat Genet 21, 414-419.

Kim, J., Yeon, J., Choi, S.K., Huh, Y.H., Fang, Z., Park, S.J., Kim, M.O., Ryoo, Z.Y., Kang, K., Kweon, H.S., et al. (2015). The Evolutionarily Conserved LIM Homeodomain Protein LIM-4/LHX6 Specifies the Terminal Identity of a Cholinergic and Peptidergic C. elegans Sensory/Inter/Motor Neuron-Type. PLoS Genet 11, e1005480.

Kim, K. and Li, C. (2004). Expression and regulation of an FMRFamide-related neuropeptide gene family in Caenorhabditis elegans. J Comp Neurol 475, 540-550.

Kow, L.M. and Pfaff, D.W. (1988). Neuromodulatory actions of peptides. Annu Rev Pharmacol Toxicol 28, 163-188.

Lee, J.B., Yonar, A., Hallacy, T., Shen, C.H., Milloz, J., Srinivasan, J., Kocabas, A., and Ramanathan, S. (2019). A compressed sensing framework for efficient dissection of neural circuits. Nat Methods 16, 126-133.

Li, C. and Kim, K. (2014). Family of FLP Peptides in Caenorhabditis elegans and Related Nematodes. Front Endocrinol (Lausanne) 5, 150.

Li, C., Kim, K., and Nelson, L.S. (1999). FMRFamide-related neuropeptide gene family in Caenorhabditis elegans. Brain Res 848, 26-34.

Lin, J.Y., Knutsen, P.M., Muller, A., Kleinfeld, D., and Tsien, R.Y. (2013). ReaChR: a red-shifted variant of channelrhodopsin enables deep transcranial optogenetic excitation. Nat Neurosci 16, 1499-1508.

Liu, T., Kim, K., Li, C., and Barr, M.M. (2007). FMRFamide-like neuropeptides and mechanosensory touch receptor neurons regulate male sexual turning behavior in Caenorhabditis elegans. J Neurosci 27, 7174-7182.

Matsumoto, A., Toyoshima, Y., Zhang, C., Isozaki, A., Goda, K., and Iino, Y. (2024). Neuronal sensorimotor integration guiding salt concentration navigation in Caenorhabditis elegans. Proc Natl Acad Sci U S A 121, e2310735121.

Matúš, D. and Prömel, S. (2018). G Proteins and GPCRs in C. elegans Development: A Story of Mutual Infidelity. J Dev Biol 6.

McIntire, S.L., Jorgensen, E., Kaplan, J., and Horvitz, H.R. (1993). The GABAergic nervous system of Caenorhabditis elegans. Nature 364, 337-341.

Moon, K.M., Kim, J., Seong, Y., Suh, B.C., Kang, K., Choe, H.K., and Kim, K. (2021). Proprioception, the regulator of motor function. BMB Rep 54, 393-402.

Nath, R.D., Chow, E.S., Wang, H., Schwarz, E.M., and Sternberg, P.W. (2016). C. elegans Stress-Induced Sleep Emerges from the Collective Action of Multiple Neuropeptides. Curr Biol 26, 2446-2455.

Painsipp, E., Herzog, H., and Holzer, P. (2008). Implication of neuropeptide-Y Y2 receptors in the effects of immune stress on emotional, locomotor and social behavior of mice. Neuropharmacology 55, 117-126.

Park, S., Ryoo, J., and Kim, D. (2022). Neural and Genetic Basis of Evasion, Approach and Predation. Mol Cells 45, 93-97.

Pierce-Shimomura, J.T., Chen, B.L., Mun, J.J., Ho, R., Sarkis, R., and McIntire, S.L. (2008). Genetic analysis of crawling and swimming locomotory patterns in C. elegans. Proc Natl Acad Sci U S A 105, 20982-20987.

Quillet, R., Ayachi, S., Bihel, F., Elhabazi, K., Ilien, B., and Simonin, F. (2016). RF-amide neuropeptides and their receptors in Mammals: Pharmacological properties, drug

development and main physiological functions. Pharmacol Ther 160, 84-132.
Ripoll-Sanchez, L., Watteyne, J., Sun, H., Fernandez, R., Taylor, S.R., Weinreb, A., Bentley, B.L., Hammarlund, M., Miller, D.M., 3rd, Hobert, O., et al. (2023). The neuropeptidergic connectome of C. elegans. Neuron 111, 3570-3589 e3575.
Ryu, L., Cheon, Y., Huh, Y.H., Pyo, S., Chinta, S., Choi, H., Butcher, R.A., and Kim, K. (2018). Feeding state regulates pheromone-mediated avoidance behavior via the insulin signaling pathway in Caenorhabditis elegans. EMBO J 37.
Ryu, T.H., Subramanian, M., Yeom, E., and Yu, K. (2022). The prominin-like Gene Expressed in a Subset of Dopaminergic Neurons Regulates Locomotion in Drosophila. Mol Cells 45, 640-648.
Sagasti, A., Hobert, O., Troemel, E.R., Ruvkun, G., and Bargmann, C.I. (1999). Alternative olfactory neuron fates are specified by the LIM homeobox gene lim-4. Genes Dev 13, 1794-1806.
Sharma, D., Kumar, K., and Bisht, G.S. (2022). A Mini-Review on Potential of Neuropeptides as Future Therapeutics. Int J Pept Res Ther 28.
Speese, S., Petrie, M., Schuske, K., Ailion, M., Ann, K., Iwasaki, K., Jorgensen, E.M., and Martin, T.F. (2007). UNC-31 (CAPS) is required for dense-core vesicle but not synaptic vesicle exocytosis in Caenorhabditis elegans. J Neurosci 27, 6150-6162.
Stawicki, T.M., Takayanagi-Kiya, S., Zhou, K., and Jin, Y. (2013). Neuropeptides function in a homeostatic manner to modulate excitation-inhibition imbalance in C. elegans. PLoS Genet 9, e1003472.
Timmons, L., Court, D.L., and Fire, A. (2001). Ingestion of bacterially expressed dsRNAs can produce specific and potent genetic interference in Caenorhabditis elegans. Gene 263, 103-112.
Turek, M., Besseling, J., Spies, J.P., Konig, S., and Bringmann, H. (2016). Sleep-active neuron specification and sleep induction require FLP-11 neuropeptides to systemically induce sleep. Elife 5.
White, J.G., Southgate, E., Thomson, J.N., and Brenner, S. (1986). The structure of the nervous system of the nematode Caenorhabditis elegans. Philos Trans R Soc Lond B Biol Sci 314, 1-340.
Yemini, E., Lin, A., Nejatbakhsh, A., Varol, E., Sun, R., Mena, G.E., Samuel, A.D.T., Paninski, L., Venkatachalam, V., and Hobert, O. (2021). NeuroPAL: A Multicolor Atlas for Whole-Brain Neuronal Identification in C. elegans. Cell 184, 272-288 e211.
Zheng, X., Chung, S., Tanabe, T., and Sze, J.Y. (2005). Cell-type specific regulation of serotonergic identity by the C. elegans LIM-homeodomain factor LIM-4. Dev Biol 286, 618-628.

## Declaration of Competing Interest

☒ The authors declare that they have no known competing financial interests or personal relationships that could have appeared to influence the work reported in this paper.

☐ The author *Click here to enter your name* is Choose an item for *Click here to enter the journal's name* and was not involved in the editorial review or the decision to publish this article.

☐The authors declare the following financial interests (e.g., any funding for the research project)/personal relationships (e.g., the author is an employee of a profitable company) which may be considered as potential competing interests:

Click here to enter your full declaration